

Article

Multiphase Equilibrium Relationships between Copper Matte and CaO-Al₂O₃-Bearing Iron Silicate Slags in Combined Smelting of WEEE and Copper Concentrates

Miao Tian ¹, Qiongqiong Wang ¹, Songsong Wang ^{1,*}, Xingbang Wan ², Qinmeng Wang ¹ and Xueyi Guo ¹

¹ School of Metallurgy and Environment, Central South University, Changsha 410083, China; miaotian2016@126.com (M.T.); qqwang0112@163.com (Q.W.); qmwang@csu.edu.cn (Q.W.); xyguo@csu.edu.cn (X.G.)

² School of Energy Science and Engineering, Central South University, Changsha 410083, China; xingbangwan@126.com

* Correspondence: songswang@csu.edu.cn

Abstract: Waste electrical and electronic equipment (WEEE) contains various valuable metals, making it a potential secondary resource for sustainable metal usage. Pyrometallurgical smelting is an efficient technique to recycle WEEE by extracting precious metals into copper matte and removing impurities into slags. The impact of WEEE impurities such as CaO and Al₂O₃ on the phase compositions of the smelting products attracts great attention for industrial metal recovery. This study clarified the impact of CaO and Al₂O₃ on the equilibrium phase compositions of copper matte and SiO₂-saturated FeO_x-SiO₂-Al₂O₃-CaO slags. The high-temperature smelting experiments were taken at a controlled p(SO₂) of 0.1 atm and 1300 °C, followed by quenching and electron probe microanalysis. The results showed that the copper and sulfur in the smelting system were highly deported into copper matte, and their distribution in matte was enhanced by increasing CaO and Al₂O₃ concentrations introduced by WEEE. The chemical copper dissolution in slags increased with increasing matte grade but decreased by adding CaO and Al₂O₃. The iron was preferentially concentrated in slags, and higher matte grades improved the iron distribution in slags. The current experimental results enrich fundamental thermodynamic data and help optimize WEEE smelting operations for efficient recovery of valuable metals.

Keywords: WEEE; smelting; phase equilibria; copper matte; iron silicate slags



Citation: Tian, M.; Wang, Q.; Wang, S.; Wan, X.; Wang, Q.; Guo, X. Multiphase Equilibrium Relationships between Copper Matte and CaO-Al₂O₃-Bearing Iron Silicate Slags in Combined Smelting of WEEE and Copper Concentrates. *Sustainability* **2024**, *16*, 890. <https://doi.org/10.3390/su16020890>

Academic Editor: Hosam Saleh

Received: 16 December 2023

Revised: 11 January 2024

Accepted: 17 January 2024

Published: 20 January 2024



Copyright: © 2024 by the authors. Licensee MDPI, Basel, Switzerland. This article is an open access article distributed under the terms and conditions of the Creative Commons Attribution (CC BY) license (<https://creativecommons.org/licenses/by/4.0/>).

1. Introduction

Sustainable utilization of metals is a well-stressed topic facing the risk of rapid depletion of high-grade primary ores. To meet rising metal demand while lessening the exploitation of natural and nonrenewable resources, WEEE becomes an essential secondary resource for recycling copper and various precious metals [1]. Methods and industrial practices for extracting metals from WEEE have been widely investigated for industrial interests [2,3]. Copper matte, as a recycler of WEEE, has great advantages in efficiently recovering precious metals through pyrometallurgical smelting [2]. In the combined smelting of WEEE and copper concentrates, copper and precious metals from WEEE are collected into matte, and impurities such as CaO, Al₂O₃, and SiO₂ are removed to iron silicate slags [4]. However, the ongoing electrical technique makes the WEEE more and more sophisticated. The valuable metals of WEEE are deeply covered by oxide impurities and plastics, presenting significant challenges in separating metals and impurities by smelting technique [5]. The increasing amounts of CaO and Al₂O₃ inevitably affect the phase relations of the smelting products, such as increasing solid proportions and enhancing slag viscosity, which influence stable smelting operations and increase metal losses. Therefore,

phase compositions of WEEE smelting products and element distribution behavior among the phases need to be clarified for efficient recovery of valuable metals.

The metal recovery efficiency in WEEE smelting is governed by their distributions between matte and smelting slags [6]. The elemental distribution behavior is affected by various factors, including O_2 partial pressure ($p(O_2)$) and SO_2 partial pressure ($p(SO_2)$), smelting temperature, and slag compositions [7]. In previous studies, phase relationships and element distribution behavior between copper matte or copper alloy and fayalite-based slags have been widely investigated, as listed in Table 1. At the copper matte smelting system, Sineva et al. [8] measured equilibrium compositions of matte and SiO_2 -saturated FeO_x - SiO_2 slags with CaO concentrations of 1.5–18 wt% at 1200 °C in a vacuum silica ampoule. The effect of temperature and CaO concentrations on phase equilibria of matte and iron silicate slags in SiO_2 or spinel saturation was studied at $p(SO_2) = 0.25$ atm and 1200–1300 °C [9–11]. Chen et al. [12,13] examined phase equilibrium between matte and CaO-bearing FeO_x - SiO_2 slags at spinel saturation and clarified the distributions of trace elements (Ag, Sn, In, and Co) in all phases at 1250 °C and $p(SO_2) = 0.25$ atm. Sun et al. [14] investigated the impact of CaO concentration on the liquidus temperature of spinel-saturated FeO - SiO_2 slags at target $p(SO_2)$ of 0.3 and 0.6 atm at a given matte grade of 72 wt% in the smelting system.

Table 1. Investigation of phase relations in copper matte smelting in literature.

Investigators	Slag Type	Additive Concentration	Temperature/°C	$p(SO_2)$ /atm	Refs.
Matte and FeO_x - SiO_2 -CaO(- Al_2O_3) slag system					
Present study	SiO_2 -sat.	5–10 wt%CaO + 5 wt% Al_2O_3	1300	0.1	-
Sineva et al.	SiO_2 -sat.	1.5, 6, 9, 18 wt% CaO	1200	$10^{-6.9}$ – $10^{-6.5}$	[8]
Fallah-Mehrjardi et al.	SiO_2 -sat.	1–4 wt% CaO	1200	0.25	[8]
Sineva et al.	SiO_2 -sat.	2.4, 3.8 wt% CaO	1300	0.25	[10]
Sineva et al.	Spinel-sat.	2.5, 4 wt% CaO	1200	0.25	[11]
Chen et al.	Spinel-sat.	4–7 wt% CaO	1250	0.25	[12]
Sun et al.	Spinel-sat.	0–6 wt% CaO	1180–1250	0.3, 0.6	[14]
Chen et al.	SiO_2 -sat.	8 wt%CaO + 8 wt% Al_2O_3	1300	0.1, 0.5	[15,16]
Sukhomlinov et al.	SiO_2 -sat.	5 wt%CaO + 5 wt% Al_2O_3	1300	0.1	[17]
Copper alloy and FeO_x - SiO_2 -CaO(- Al_2O_3) slag system					
Heo et al.	SiO_2 -sat.	2–6 wt% CaO	1200	$p(O_2) = 10^{-10}$	[18]
	SiO_2 -sat.	3 wt%CaO + 1–10 wt% Al_2O_3	1200	$p(O_2) = 10^{-10}$	
Kim et al.	SiO_2 -sat.	4.4 wt%CaO + (4.4 wt% Al_2O_3)	1250	$p(O_2) = 10^{-10}$ – 10^{-4}	[19]
Avarmaa et al.	Spinel-sat.	5 wt%CaO + 20 wt% Al_2O_3	1300	$p(O_2) = 10^{-10}$ – 10^{-5}	[5]

Concerning the FeO - SiO_2 -CaO- Al_2O_3 slag system, the effect of CaO and Al_2O_3 on equilibrium phase relations between matte and SiO_2 -saturated slags was researched by Chen et al. [15,16] and Sukhomlinov et al. [17] at 1300 °C and controlled $p(SO_2)$ of 0.1 and 0.5 atm. Phase relations and element distributions between copper alloy and FeO_x - SiO_2 - Al_2O_3 -CaO slags at SiO_2 saturation or spinel saturation in black copper smelting conditions were reported in experimental observations [5,18,19]. In industrial WEEE smelting, the sources and complexity of WEEE imported into the smelting system can lead to higher impurity concentrations, changing the slag properties, and increasing metal loss in slags. To improve the recovery efficiency of valuable elements, the effect of smelting conditions and additional impurities on phase compositions and element distribution deserves further research.

This study aims to investigate the phase equilibrium relationship of copper matte and FeO_x - SiO_2 - Al_2O_3 -CaO slags for WEEE recycling through copper matte smelting processes. High-temperature experiments were conducted to measure equilibrium compositions of copper matte and SiO_2 -saturated slags with different additions of CaO and Al_2O_3 for target matte grades of 55–75 wt% at 1300 °C and $p(SO_2) = 0.1$ atm. The element distribution coefficient between the matte and slags was calculated using the experimental measurements. Based on the current findings, the combined effect of CaO and Al_2O_3 on

smelting products could be quantified. The observations in the current study could enrich thermodynamic data and help regulate WEEE smelting operations.

2. Materials and Methods

The initial copper matte mixtures were prepared by combining the high purity of Cu_2S and FeS in weight ratios of $\text{Cu}_2\text{S}/\text{FeS} = 70/30$ for target matte grade ranges of 55 to 70 wt% and $\text{Cu}_2\text{S}/\text{FeS} = 80/20$ for a fixed matte grade of 75 wt% to shorten the required equilibration time [15]. The slag mixtures were prepared using Fe_2O_3 (99.99 wt%, Macklin, Shanghai, China), SiO_2 (99.90 wt%, Macklin), Al_2O_3 (99.99 wt%, Aladdin, Shanghai, China), and CaO (99.90 wt%, Aladdin) in weight ratios of $\text{Fe}_2\text{O}_3/\text{SiO}_2/\text{Al}_2\text{O}_3/\text{CaO} = 40/50/5/5$ and $31/54/5/10$, respectively. In each experiment, approximately 0.1 g of the sulfide mixtures and the same amount of slag mixtures and metallic copper powder (99.999 wt%, Alfa Aesar, Shanghai, China) were weighted and equilibrated. The metallic copper was transformed to copper matte in the smelting conditions, which will be reported in further publication.

The starting materials were thoroughly mixed and pressed into a 5-millimeter tablet. The sample pellet was placed into a SiO_2 crucible and hung in the hot zone of a vertical tube furnace ($L \times \text{O.D.} = 1000 \times 60$ mm, SGL-1700C, Jujing, China) by a Kanthal A1 wire, as shown in Figure 1. The sample was annealed at 1300°C and $p(\text{SO}_2) = 0.1$ atm for 8 h to obtain uniform phase compositions, as proposed in the previous study [20]. The furnace temperature was regulated by a PID controller. The sample temperature was monitored by a measuring thermocouple placed beside the sample. The $p(\text{O}_2)$, $p(\text{S}_2)$, and $p(\text{SO}_2)$ inside the reaction tube were controlled to achieve target matte grades by regulating gas flowrates of CO (99.90 vol%), CO_2 (99.99 vol%), SO_2 (99.90 vol%), and Ar (99.999 vol%), which were predicted by thermodynamic software FactSage 7.1 and presented in Table 2 [20].

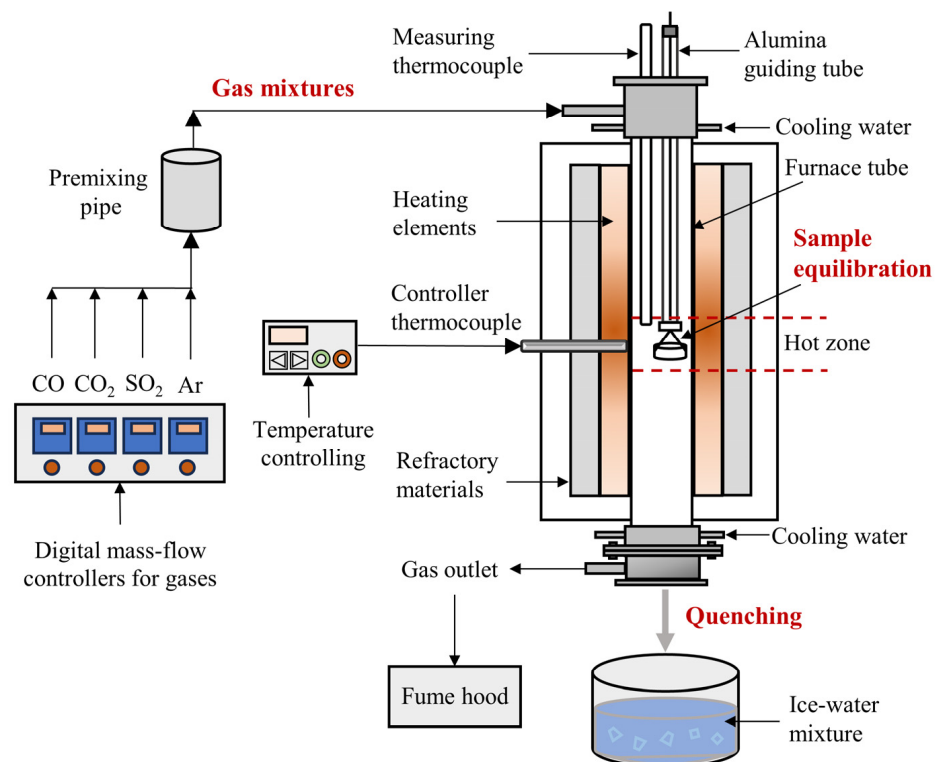


Figure 1. Schematic diagrams of the reaction furnace and high-temperature experiments.

Table 2. The predicted gas flow rates for the target smelting atmosphere at 1300 °C and $p(\text{SO}_2) = 0.1$ atm.

Target Matte Grade (Cu-wt%)	Target $\lg[p(\text{O}_2)/P^\ominus]$	Target $\lg[p(\text{S}_2)/P^\ominus]$	Gas Flowrate (mL/min)			
			CO	CO ₂	SO ₂	Ar
55	−8.14	−2.11	27	67	47	259
60	−8.07	−2.26	22	68	45	265
65	−7.96	−2.48	16	71	43	270
70	−7.80	−2.79	11	72	42	275
75	−7.58	−3.23	8	74	41	278

After equilibration, the samples were directly quenched into an ice-water mixture to attain phase assembly at high temperatures. Subsequently, the samples were mounted, polished, and carbon-coated for analysis. The microstructures of the samples were observed by SEM-EDS. The element concentrations in all phases were detected by EPMA-WDS at an accelerating voltage of 15 kV and a beam current of 20 nA. The beam diameter was 20 μm for the matte and liquid slag phases and 5 μm for the solid tridymite.

The standard materials used for EPMA measurements were Cu (Cu-K α), Fe (Fe-K α) for matte, Hematite (Fe-K α) for slag, FeS₂ (S-K α), Al₂O₃ (Al-K α), CaSiO₃ (Ca-K α), Quartz (Si-K α , O-K α in matte), and Obsidian (O-K α) for slag. The EPMA detection limits for elements in different phases are listed in Table 3. For each sample, at least 8–10 points were randomly selected from each phase to obtain reliable measurements. The slag compositions were calculated as FeO, SiO₂, CaO, and Al₂O₃ for ease of presentation.

Table 3. Element detection limits of EPMA in different phases (ppm).

Element	Cu	Fe	S	O	Si	Al	Ca
In Matte	309	185	98	206	67	56	119
In Liquid slag	219	141	73	334	70	51	103
In Tridymite	179	119	71	361	80	49	82

3. Results and Discussion

3.1. Microstructures of Matte and Tridymite-Saturated Slags

Typical microstructures of equilibrium phases of matte and SiO₂-saturated FeO_x-SiO₂-CaO-Al₂O₃ slags obtained at 1300 °C and $p(\text{SO}_2) = 0.1$ atm are shown in Figure 2. The phases consist of liquid matte, liquid slag, and tridymite crystals in all samples within the matte grades of 55–75 wt% in the equilibrium system. Thin copper-rich veins existed in the matte phase during the quenching process, as seen in Figure 2c. Solid tridymite particles were precipitated discretely in the liquid slag, and some small particles existed on the slag-crucible interfaces.

3.2. Matte Composition

The measured matte compositions with standard deviations are shown in Table 4. The elements of the matte phase include Cu, Fe, and S. The original total amount presents the unnormalized total elemental concentrations detected by EPMA, which were within 97.08–100.66 wt%.

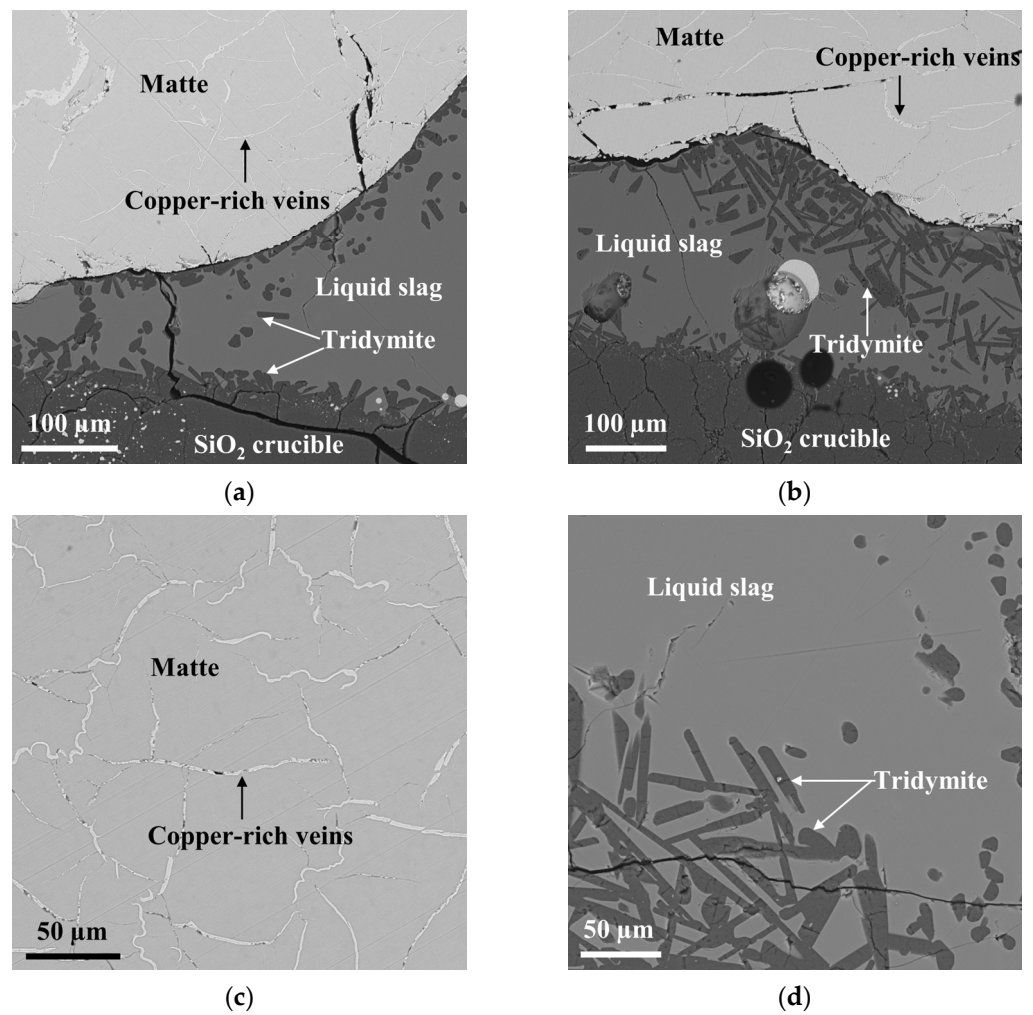


Figure 2. Microstructures of matte/slag/tridymite equilibria at 1300 °C and $p(\text{SO}_2) = 0.1$ atm. (a) Sample 4: 62.17 wt% Cu in matte with $\text{FeO}_x\text{-SiO}_2\text{-Al}_2\text{O}_3\text{-5 wt% CaO}$ slags; (b) Sample 13: 66.39 wt% Cu in matte with $\text{FeO}_x\text{-SiO}_2\text{-Al}_2\text{O}_3\text{-10 wt% CaO}$ slags; (c) Magnified matte with copper-rich veins; (d) Liquid slag with solid tridymite particles.

Table 4. Experimentally determined matte compositions of matte/tridymite/ $\text{FeO}_x\text{-SiO}_2\text{-Al}_2\text{O}_3\text{-CaO}$ slag equilibrium system at 1300 °C and $p(\text{SO}_2) = 0.1$ atm.

Sample No.	$\lg[p(\text{O}_2)/P^0]$	Normalized Matte Composition (wt%)				Original Total Amount (wt%)
		Cu	Fe	S	O	
1	−8.14	59.90 ± 0.60	14.18 ± 0.43	23.88 ± 0.47	1.02 ± 0.23	99.20 ± 0.35
2	−8.14	61.19 ± 0.17	13.26 ± 0.38	24.80 ± 0.47	0.47 ± 0.20	99.64 ± 0.77
3	−8.07	61.66 ± 0.35	13.01 ± 0.40	23.91 ± 0.43	0.83 ± 0.33	98.14 ± 0.55
4	−8.07	62.17 ± 0.37	12.64 ± 0.14	24.04 ± 0.39	0.78 ± 0.14	98.87 ± 0.57
5	−7.96	68.60 ± 0.52	7.92 ± 0.46	22.07 ± 0.47	0.59 ± 0.15	100.51 ± 0.34
6	−7.96	69.12 ± 0.98	7.51 ± 0.76	22.12 ± 0.31	0.54 ± 0.19	100.66 ± 0.66
7	−7.8	72.74 ± 0.12	4.42 ± 0.10	20.35 ± 0.13	0.52 ± 0.04	99.54 ± 0.42
8	−7.8	73.73 ± 0.18	3.95 ± 0.14	20.14 ± 0.13	0.45 ± 0.04	98.46 ± 0.38
9	−7.58	75.54 ± 0.15	2.41 ± 0.05	19.67 ± 0.15	0.53 ± 0.04	97.68 ± 0.31
10	−7.58	75.73 ± 0.18	2.27 ± 0.10	19.91 ± 0.11	0.36 ± 0.04	97.08 ± 0.34
11	−8.14	63.11 ± 0.29	12.09 ± 0.35	23.83 ± 0.19	0.72 ± 0.10	97.82 ± 0.37
12	−8.14	63.98 ± 0.23	11.40 ± 0.26	23.55 ± 0.15	0.81 ± 0.10	99.41 ± 0.40
13	−8.07	66.39 ± 0.35	9.51 ± 0.44	23.17 ± 0.17	0.59 ± 0.06	97.10 ± 0.54
14	−8.07	66.58 ± 0.42	9.44 ± 0.10	23.09 ± 0.33	0.54 ± 0.06	98.84 ± 0.25

Table 4. Cont.

Sample No.	$\lg[p(\text{O}_2)/P^0]$	Normalized Matte Composition (wt%)				Original Total Amount (wt%)
		Cu	Fe	S	O	
15	−7.96	70.01 ± 0.80	6.76 ± 0.47	21.73 ± 0.22	0.70 ± 0.16	99.16 ± 0.47
16	−7.96	73.49 ± 0.39	3.94 ± 0.28	19.66 ± 0.22	0.60 ± 0.09	98.68 ± 0.45
17	−7.8	74.07 ± 0.23	3.76 ± 0.13	20.82 ± 0.13	0.38 ± 0.06	99.82 ± 0.44
18	−7.8	75.32 ± 0.69	2.76 ± 0.42	19.59 ± 0.27	0.35 ± 0.25	99.65 ± 0.71
19	−7.58	76.11 ± 0.17	1.98 ± 0.06	19.51 ± 0.13	0.47 ± 0.02	97.92 ± 0.41
20	−7.58	76.23 ± 0.24	2.02 ± 0.12	19.65 ± 0.11	0.29 ± 0.13	98.19 ± 0.38

Figure 3 shows the concentration of Cu, Fe, S, and O against the prevailing oxygen partial pressure, or matte grade, in this study. The experimental data in the literature [15,17] for 1300 °C and $p(\text{SO}_2) = 0.1$ atm were presented in the graphs of Figure 3 for comparison. In Figure 3a, the Cu concentration in matte increased with increasing oxygen partial pressure. At a given $p(\text{O}_2)$ of $10^{-8.14}$ atm, matte grade was improved from 59.90 wt% to 63.11 wt% when CaO concentration in tridymite-saturated $\text{FeO}_x\text{-SiO}_2\text{-Al}_2\text{O}_3\text{-CaO}$ slags rose from approximately 5 wt% to 10 wt%. When the matte composition is close to white matte (Cu_2S), adding CaO has little effect on matte grade.

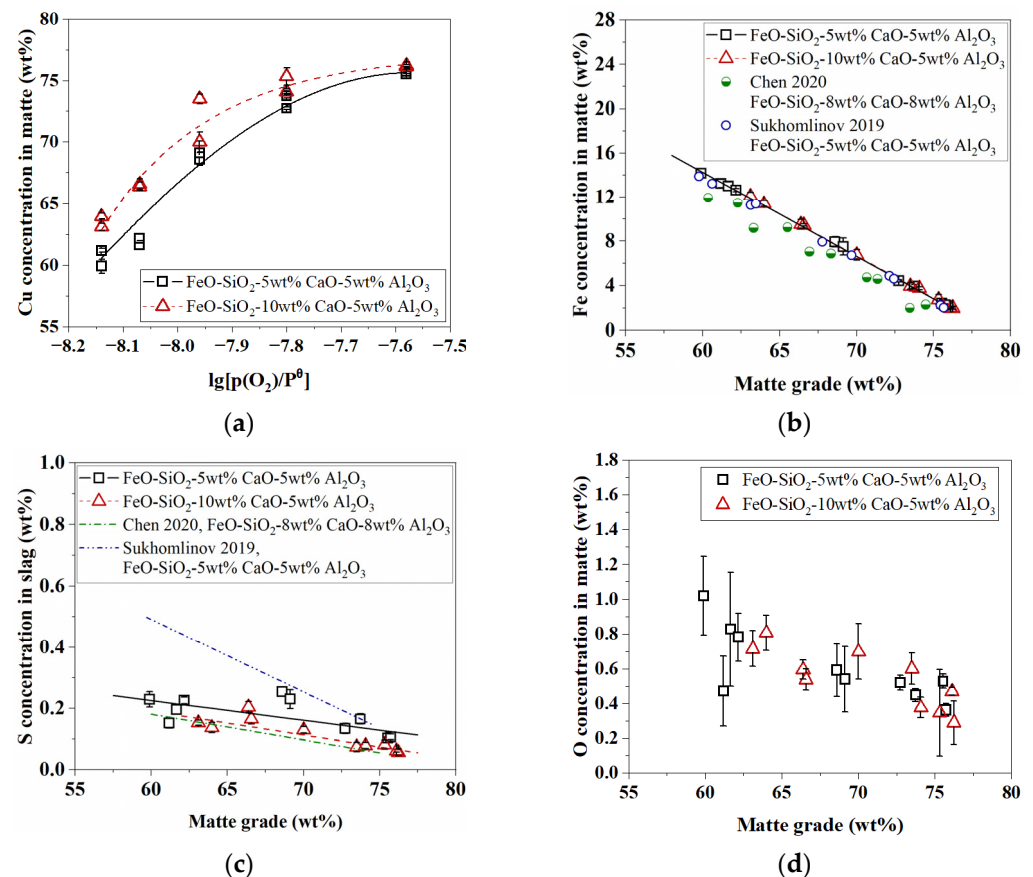


Figure 3. (a) Copper concentration in matte against oxygen partial pressure at 1300 °C and $p(\text{SO}_2) = 0.1$ atm; (b) Iron, (c) sulfur, and (d) oxygen concentrations in matte as a function of matte grade in this study and literature [15,17].

Similarly, Chen et al. [15] and Sukhomlinov et al. [17] found that adding slag modifiers to tridymite-saturated slags, such as CaO and Al₂O₃, led to an increasing matte grade at a fixed $p(\text{O}_2)$ at 1300 °C and $p(\text{SO}_2) = 0.1$ atm. The addition of CaO and Al₂O₃ in slags decreased the FeO activity of fayalite-based $\text{FeO}_x\text{-SiO}_2$ slags, and as a result, the FeS in matte oxidized into the slags [21]. Meanwhile, the matte grade got enhanced with the

decreasing iron concentration in matte. Similarly, the basic oxides like MgO also led to a decrease in the FeO activity of slags, thus improving the matte grade, as suggested by Abdeyazdan et al. [22] and our previous study [20].

As can be seen in Figure 3b,c, Fe and S concentrations in matte decreased with increasing matte grade, independently from the increasing CaO in the tridymite-saturated $\text{FeO}_x\text{-SiO}_2\text{-Al}_2\text{O}_3\text{-CaO}$ slags. In the literature, the Fe and S concentrations showed similar downward trends against the matte grade and were not affected by adding CaO, Al_2O_3 , and MgO in slags. The oxygen dissolution in matte displayed the opposite trend with the increasing matte grade (Figure 3d), as iron had a stronger chemical affinity for oxygen than copper [23]. The presence of CaO had no apparent impact on oxygen concentration in matte, showing good agreement with the previous data [15,17].

3.3. Slag Composition and Isotherms

3.3.1. Slag Composition

The experimentally measured liquid slag compositions with standard deviations of the tridymite-saturated $\text{FeO}_x\text{-SiO}_2\text{-Al}_2\text{O}_3\text{-CaO}$ system are listed in Table 5. The liquid slag contained FeO, SiO_2 , Al_2O_3 , CaO, and chemically dissolved Cu and S. The slag compositions against matte grade with different CaO additions are presented in Figure 4. The experimentally determined data by Chen et al. [15] and Sukhomlinov et al. [17] were also plotted in the graphs to compare the variation of slag compositions with different additions of Al_2O_3 and CaO.

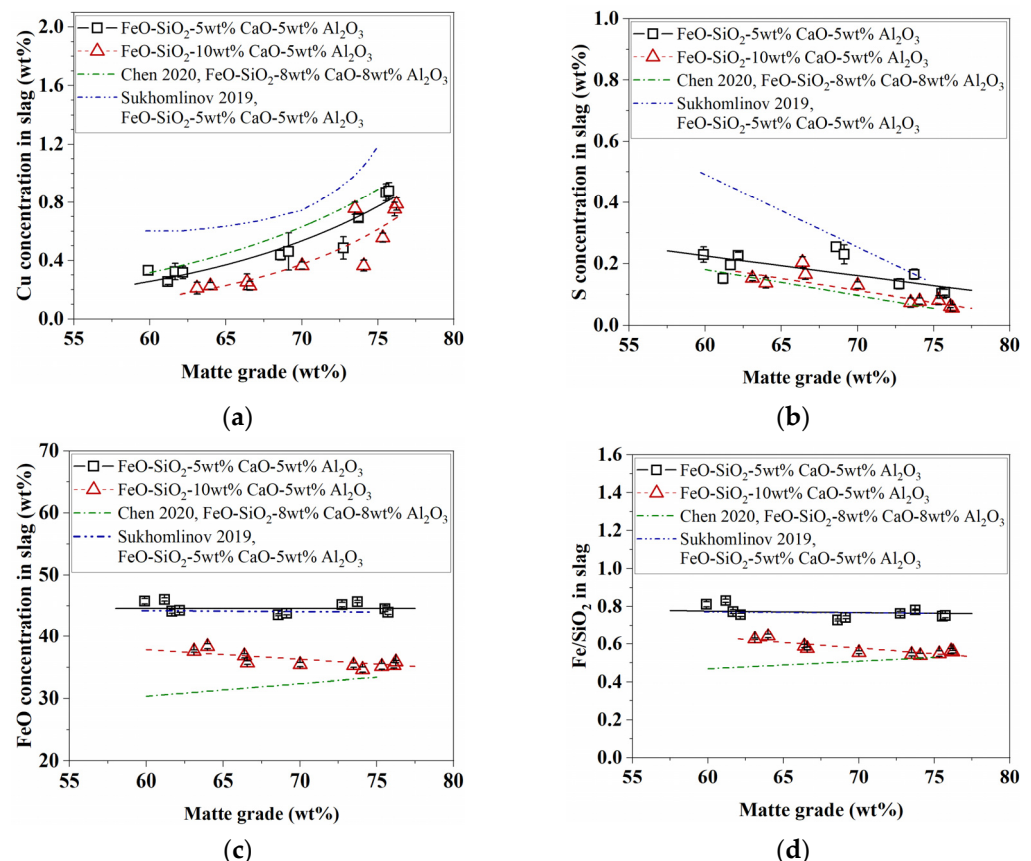


Figure 4. Slag composition against matte grade at 1300 °C and $p(\text{SO}_2) = 0.1$ atm. (a) Copper concentration in slags; (b) Sulfur concentration in slags; (c) FeO concentration in slags; (d) Fe/SiO₂ mass ratio of slags in this study and literature [15,17].

Table 5. Experimentally measured slag compositions of matte/tridymite/FeO_x-SiO₂-Al₂O₃-CaO slag equilibrium system at 1300 °C and p(SO₂) = 0.1 atm.

Sample No.	Normalized Slag Composition (wt%)				Original Total Amount (wt%)	Cu in Slag (wt%)	S in Slag (wt%)
	Al ₂ O ₃	CaO	SiO ₂	FeO			
1	4.71 ± 0.50	5.61 ± 0.11	43.89 ± 0.42	45.79 ± 0.43	98.87 ± 0.67	0.33 ± 0.03	0.23 ± 0.03
2	5.14 ± 0.28	5.70 ± 0.29	43.11 ± 0.31	46.05 ± 0.26	98.94 ± 0.68	0.25 ± 0.02	0.15 ± 0.02
3	5.91 ± 0.32	5.48 ± 0.23	44.46 ± 0.37	44.16 ± 0.32	99.22 ± 0.57	0.32 ± 0.06	0.20 ± 0.01
4	4.76 ± 0.23	5.44 ± 0.12	45.52 ± 0.30	44.28 ± 0.27	99.02 ± 0.47	0.32 ± 0.04	0.23 ± 0.01
5	5.59 ± 0.05	4.33 ± 0.08	46.51 ± 0.17	43.56 ± 0.16	99.30 ± 0.34	0.44 ± 0.03	0.25 ± 0.02
6	5.80 ± 0.08	4.46 ± 0.05	45.90 ± 0.23	43.83 ± 0.25	98.71 ± 0.54	0.46 ± 0.13	0.23 ± 0.03
7	4.49 ± 0.16	4.23 ± 0.14	46.05 ± 0.34	45.23 ± 0.34	97.96 ± 0.26	0.49 ± 0.08	0.13 ± 0.02
8	4.76 ± 0.25	4.10 ± 0.10	45.43 ± 0.13	45.70 ± 0.18	98.72 ± 0.36	0.69 ± 0.02	0.17 ± 0.02
9	5.09 ± 0.15	4.07 ± 0.11	46.29 ± 0.53	44.55 ± 0.46	98.40 ± 0.48	0.87 ± 0.06	0.10 ± 0.01
10	5.49 ± 0.08	5.05 ± 0.25	45.47 ± 0.39	43.99 ± 0.36	98.17 ± 0.56	0.88 ± 0.06	0.11 ± 0.01
11	5.74 ± 0.20	10.00 ± 0.14	46.67 ± 0.15	37.59 ± 0.17	98.56 ± 0.25	0.21 ± 0.04	0.15 ± 0.01
12	5.58 ± 0.39	9.62 ± 0.13	46.45 ± 0.34	38.34 ± 0.39	98.39 ± 0.68	0.23 ± 0.02	0.14 ± 0.02
13	5.34 ± 0.12	9.16 ± 0.29	48.68 ± 0.35	36.82 ± 0.33	99.26 ± 0.42	0.25 ± 0.05	0.20 ± 0.02
14	5.76 ± 0.29	10.27 ± 0.12	48.26 ± 0.28	35.71 ± 0.29	99.10 ± 0.32	0.23 ± 0.03	0.17 ± 0.02
15	5.44 ± 0.16	9.46 ± 0.17	49.66 ± 0.27	35.44 ± 0.34	99.15 ± 0.52	0.36 ± 0.02	0.13 ± 0.01
16	4.94 ± 0.12	9.36 ± 0.20	50.40 ± 0.38	35.30 ± 0.35	99.68 ± 0.24	0.76 ± 0.04	0.07 ± 0.01
17	5.12 ± 0.07	10.23 ± 0.14	50.03 ± 0.50	34.62 ± 0.42	98.60 ± 0.33	0.37 ± 0.04	0.08 ± 0.01
18	5.02 ± 0.26	9.99 ± 0.07	49.86 ± 0.65	35.13 ± 0.46	98.77 ± 0.32	0.56 ± 0.03	0.08 ± 0.02
19	5.13 ± 0.21	10.76 ± 0.20	48.80 ± 0.55	35.31 ± 0.43	98.57 ± 0.35	0.75 ± 0.05	0.06 ± 0.00
20	4.83 ± 0.26	9.29 ± 0.30	50.02 ± 0.39	35.86 ± 0.18	98.09 ± 0.87	0.79 ± 0.04	0.06 ± 0.01

Figure 4a shows that the dissolved copper in tridymite-saturated FeO_x-SiO₂-Al₂O₃-CaO slags had an increasing trend with increasing matte grade at a fixed CaO concentration under 1300 °C and p(SO₂) = 0.1 atm. Adding CaO to the smelting slag decreased the chemical copper dissolution in slags at all matte grades. At a fixed matte grade of around 70 wt%, copper losses in slags reduced from 0.46 wt% to 0.36 wt% when CaO concentrations in the slag were increased from 5 wt% to 10 wt%. Under the same conditions in the literature, copper loss in slags decreased by improving concentrations of CaO from 5 wt% [15] to 8 wt% [17], showing good agreement with this study. The positive impact of CaO on reducing copper loss can be explained by replacing copper cations in slags with Ca²⁺ [19]. In industry, copper loss in copper matte smelting slags results from chemical dissolution and physical entrainment. The entrained copper droplets in slags could also be reduced by CaO modification. The polymeric silicate networks of the slag dissociated by adding CaO, decreasing the slag viscosity and lowering mechanical copper entrainment [19].

Figure 4b presents the sulfur solubility in slags against matte grade for selected CaO and Al₂O₃ concentrations in slags. The dissolved sulfur concentration in slags at tridymite saturation is inversely associated with matte grade. In this study, when the CaO and Al₂O₃ concentrations in slags were both 5 wt%, the sulfur concentration in slags was found to reduce from around 0.2 wt% to 0.1 wt%, while the matte grade was improved from 59.90 wt% to 75.73 wt%. By increasing the CaO concentration in slags to 10 wt% under the same conditions as in this study, the sulfur solubility in slags decreased from around 0.1 wt% to 0.06 wt% at a fixed matte grade of approximately 76 wt%. The presence of CaO could reduce the sulfur dissolution in slags, which agrees well with observations in the literature [15,17].

As shown in Figure 4c, FeO concentration in tridymite-saturated slags fluctuated around 45 wt% with fixed CaO and Al₂O₃ additions of 5 wt% in the present study within matte grades of 60–76 wt%. As the CaO addition in slags increased to 10 wt%, the FeO concentration of the slag displayed a downward trend with increasing matte grade. However, the decrease in FeO concentration was only by 2–3 wt% over the entire matte grade range of 63–76 wt%. At a fixed matte grade, adding CaO and Al₂O₃ led to a remarkable decrease in the FeO concentration of tridymite-saturated slags. Chen et al. [15] and Sukhomlinov et al. [17] reported similar trends of FeO in slags with different concentra-

tions of CaO and Al₂O₃. This tendency can be explained by the decrease in FeO activity in slags resulting from increasing amounts of the slag modifiers CaO and Al₂O₃ [23].

The Fe/SiO₂ weight ratios of the SiO₂-saturated slags showed constant values, while the matte grade varied. As the CaO concentration of the FeO_x-SiO₂-Al₂O₃-CaO slags increased from 5 wt% to 10 wt%, the Fe/SiO₂ ratio of the slags in this study decreased from approximately 0.8 to 0.6. Similarly, under the same smelting conditions of 1300 °C and p(SO₂) = 0.1 atm, the results from the literature showed that the Fe/SiO₂ of slags reduced from around 0.8 to 0.5 by increasing CaO and Al₂O₃ concentrations of slags from 5 wt% to 8 wt% [15,17]. The results illustrate that more SiO₂ flux is required for the tridymite-saturated iron silicate slags with higher levels of CaO and Al₂O₃ [10].

Typical industrial slag compositions of copper matte smelting processes are summarized in Table 6 for comparison. In flash smelting, copper loss in slags was approximately 0.5–0.6 wt% [6]. In Noranda continuous copper matte smelting, copper loss in slags achieved 5 wt% for a matte grade of 78.5 wt% [24]. The copper concentration in smelting slags produced from oxygen bottom-blown smelting was 3.16 wt% at a fixed matte grade of 70.83% [25]. In the Ausmelt smelting system, copper matte and smelting slags were produced in a top submerged lance (TSL) smelting furnace. The smelting products were then delivered to an electrical settling furnace to separate matte and slags [26]. The copper loss in the slags collected from the Tongling Ausmelt TSL smelting system was 0.6–0.8 wt% [26].

Table 6. Typical slag compositions in industrial copper matte smelting processes.

Technique	Matte Grade (wt%)	Slag Composition (wt%)						Temperature (°C)	Ref.
		Cu	S	Fe	SiO ₂	CaO	Al ₂ O ₃		
Present study	60–76	0.25–0.88	0.10–0.25	46	45	5	5	1300	
Present study	63–76	0.21–0.79	0.06–0.20	38	50	10	5	1300	
Inco flash smelting	-	0.62	1.1	39	37.1	1.73	4.72	1250	[6]
Outokumpu flash smelting	64.9	0.53	1.2	38.7	29.7	1.2	-	1250	[6]
Noranda continuous smelting	78.5	5.0	1.7	38.2	23.1	1.5	5.0	1200	[24]
Oxygen bottom-blown smelting	70.83	3.16	0.86	42.58	25.24	-	-	1200	[25]
Tongling Ausmelt smelting	48–52	0.6–0.8	-	-	-	-	-	1250–1300	[26]

The experimentally measured copper loss in slags in the present study derives from chemical copper dissolution. The copper losses in industrial smelting slags are caused by chemical dissolution and physical entrainment [21]. The physical copper losses in slags depend on slag properties and smelting operations, such as slag viscosity, slag saturation type, slag fluidity, the proportion of solids in slags, and slag residence time [6,26]. While industrial smelting operations vary, the mechanical copper loss in slag can account for 65–80% of the total copper loss [6]. In practice, the smelting operations and slag compositions could be optimized to reduce mechanical copper loss by providing sufficient residence time and decreasing the solid proportion in the slag.

3.3.2. Slag Isotherms

Figure 5 presents the isothermal sections of the FeO_x-SiO₂-Al₂O₃-CaO slag system with CaO concentrations of 5 wt% and 10 wt% under fixed p(SO₂) of 0.1 atm, p(O₂) of 10⁻⁸ atm, and 1300 °C. The slag phase diagram was predicted by FactSage 7.1 using the “PhaseDiagram” module. The databases selected for calculations were “FactPS” and “FToxide”. The solutions “FToxid-SLAGA”, “FToxid-SPINA”, “FToxid-MeO”, “FToxid-cPyrA”, “FToxid-Mull”, “FToxid-CORU”, “FToxid-WOLLA”, “FToxid-aC2SA”, “FToxid-Mel_A”, and “FToxid-OlivA” were utilized to predict the isotherms of the slags. The experimentally measured slag compositions in the present study were also projected on the 1300 °C isotherms of FeO_x-SiO₂-Al₂O₃-CaO slags.

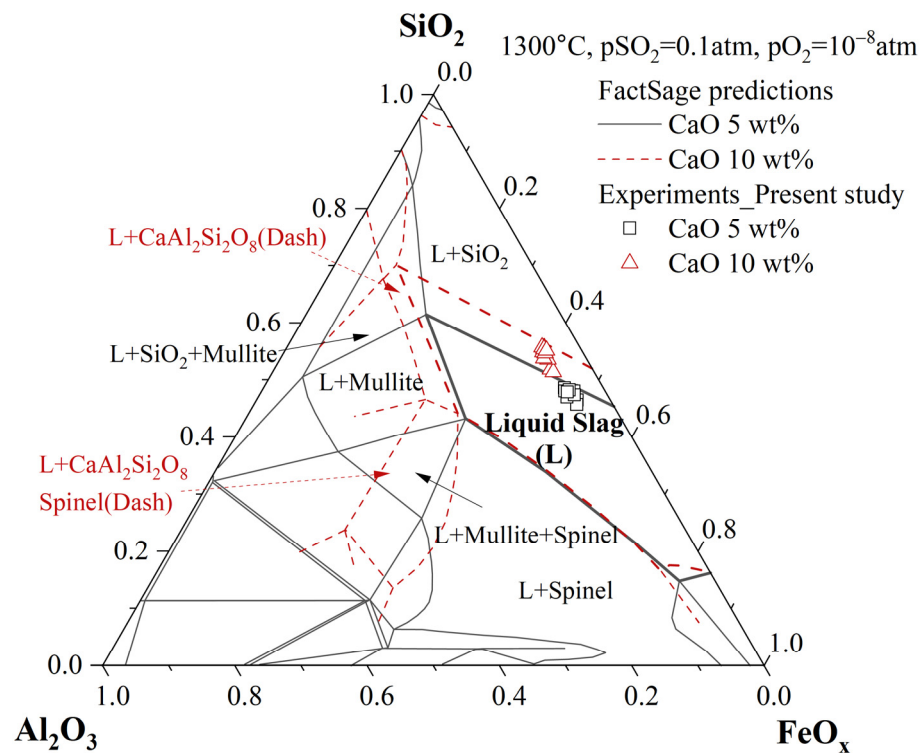


Figure 5. An isotherm section of superimposed phase diagrams of $\text{FeO}_x\text{-SiO}_2\text{-Al}_2\text{O}_3$ systems with CaO of 5 wt% (black solid line) and 10 wt% (red dash line), respectively.

As displayed in Figure 5, the predicted liquid domain of the $\text{FeO}_x\text{-SiO}_2\text{-Al}_2\text{O}_3\text{-CaO}$ slags at $p(\text{O}_2)$ of 10^{-8} atm and 1300°C was restricted by the generation of solid SiO_2 and spinel, depending on the Fe/ SiO_2 ratio of the slags. The solubility of Al_2O_3 in the slag system was limited by the formation of mullite and $\text{CaAl}_2\text{Si}_2\text{O}_8$ with CaO concentrations in slags of 5 wt% and 10 wt%, respectively. With the increasing CaO concentration in slags, the SiO_2 primary phase field extended to an area with a higher SiO_2 concentration but lower FeO, whereas the spinel primary phase field and mullite or $\text{CaAl}_2\text{Si}_2\text{O}_8$ primary phase field had no obvious changes. The experimentally observed slag compositions fit well with the calculated SiO_2 -slag phase boundaries at CaO addition of 5 wt% and 10 wt%, respectively. Increasing the CaO concentration of the fayalite-based $\text{FeO}_x\text{-SiO}_2$ slags would increase SiO_2 concentration on the SiO_2 -saturated line and lower the liquidus temperature. In industrial smelting, adding CaO in slags could help dissolve crystallized solid SiO_2 into liquid slag, maintain a slag with low proportions of solids for low slag viscosity, and reduce entrained metal loss in slags.

3.4. Distributions of Cu, Fe, and S

The element recovery efficiency in smelting was determined by their distribution behavior between matte and slags. The distribution coefficient could be used to describe the department tendency of copper, iron, and sulfur in smelting processes, as formulated in Equation (1):

$$L^{m/s}(E) = \frac{w(E)_{\text{matte}}}{w(E)_{\text{slag}}}, \quad (1)$$

where $L^{m/s}(E)$ refers to the calculated distribution coefficient of element (E) between matte and slag, and $w(E)$ refers to the element (E) concentration in matte and slag measured by EPMA.

The distribution coefficients of copper and iron between the matte and slag decreased with the increasing matte grade at 1300°C and $p(\text{SO}_2) = 0.1$ atm, as shown in Figure 6a,b. Adding CaO and Al_2O_3 to slags favored the copper distribution in matte. As indicated

in Figure 6a, the copper distribution coefficient between the matte and slag increased from around 200 to 300 by increasing the CaO concentration in the slags from 5 wt% to 10 wt% for the matte grade of 63 wt% in the present study. Iron was mainly deported into slags, and a higher matte grade could improve its department into slags. By increasing the CaO concentration in slags from 5 wt% to 10 wt% at a fixed matte grade of 63 wt%, the iron distribution coefficient varied from around 0.3 to 0.4 due to the lowering of the FeO concentration in slags.

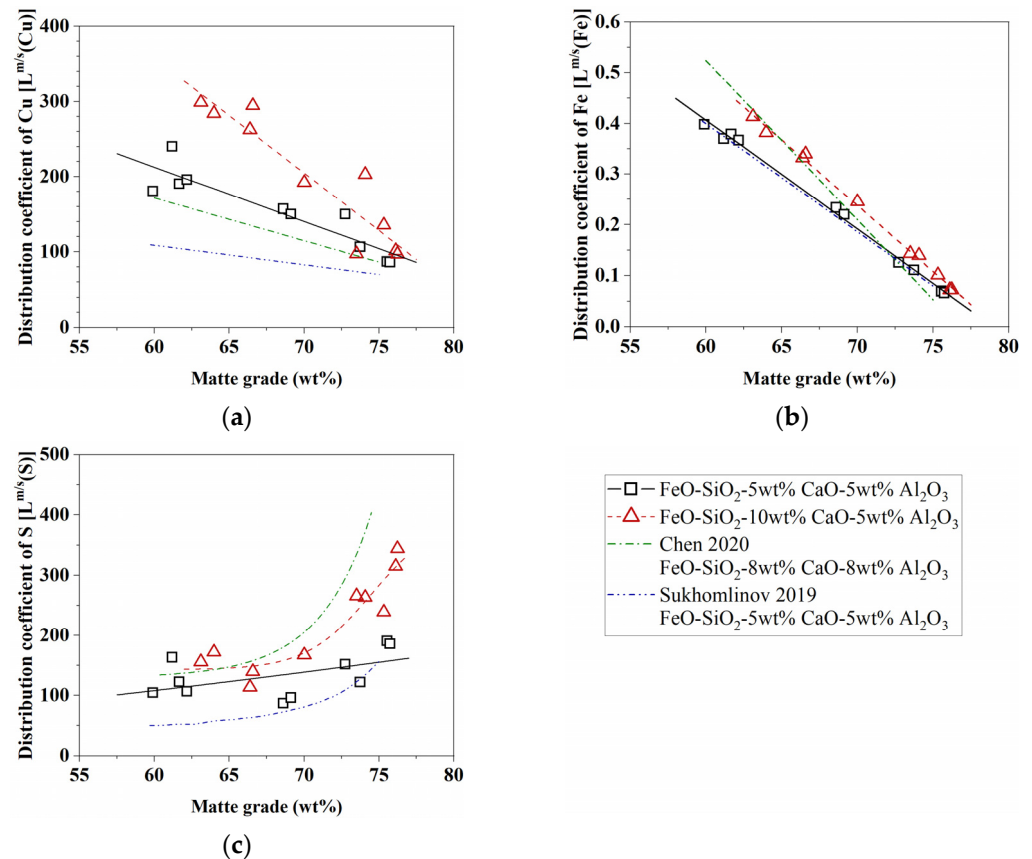


Figure 6. Distribution coefficient of (a) copper, (b) iron, and (c) sulfur against matte grade at 1300 °C and $p(SO_2) = 0.1$ atm in the present study and literature [15,17].

The sulfur distribution coefficient displayed an upward trend with the increasing matte grade, as seen in Figure 6c. Sulfur distributes preferentially into matte across the entire matte grade range investigated. Adding CaO and Al₂O₃ improves sulfur department in matte. The trend lines for distribution coefficients of Cu, Fe, and S between the matte and slags fit well with the observations by Chen et al. [15] and Sukhomlinov et al. [17] with different concentrations of CaO and Al₂O₃ in slags.

3.5. Industrial WEEE Smelting for Sustainable Metal Recovery

This investigation clarifies phase compositions and element distributions in smelting WEEE and copper concentrates for the sustainable use of valuable metals. Copper from WEEE and copper concentrates are captured into copper matte. Iron is oxidized to slag and forms an iron silicate slag with SiO₂ flux [27]. Additional impurities, like CaO and Al₂O₃, originating from WEEE and primary ores, are removed by smelting slags. In industrial smelting, optimal regulation of slag chemistry and smelting operations is crucial for the stable operation of WEEE recycling and the efficient recovery of valuable elements [28]. Based on the present results, higher oxygen partial pressure and adding CaO and Al₂O₃ to slags could improve copper concentration in matte. In contrast, the iron and sulfur concentrations in matte were reduced by the addition of slag modifiers. The chemically

dissolved copper in the slags increased with higher matte grades but was reduced by adding CaO and Al₂O₃. In general, copper and sulfur were highly distributed in matte, and lower matte grades and additions of CaO and Al₂O₃ improved their department into matte. On the contrary, iron was predominantly deported into slags with an increasing matte grade.

Moreover, mechanical entrainment loss of metals in slags caused by high slag viscosity is inevitable. With increasing amounts of CaO and Al₂O₃ introduced in slags, solid tridymite, spinel, or mullite would crystallize in liquid slag and increase slag viscosity. To reduce physical entrainment of metals in slags, the slag compositions should be maintained in a full liquid region for good fluidity based on the FeO_x-SiO₂-Al₂O₃-CaO slag phase diagram. The Fe/SiO₂ ratio and concentrations of CaO and Al₂O₃ in slags could be adjusted to limit the solid proportions in slags for low slag viscosity and metal losses [29]. Therefore, the present phase relations and element distribution data could help design fluxing strategies and optimize smelting operations for recycling WEEE.

4. Conclusions

This study provides quantitative results on phase equilibria in the combined smelting of WEEE and copper concentrates. The main products of WEEE smelting were copper matte and FeO_x-SiO₂-Al₂O₃-CaO slags. The distributions of copper, iron, and sulfur between copper matte and SiO₂-saturated iron silicate slags were experimentally determined at 1300 °C and p(SO₂) = 0.1 atm. The impact of CaO and Al₂O₃ on equilibrium phase compositions and elemental distributions of the WEEE smelting processes was clarified. In smelting WEEE and copper concentrates, Cu and S were preferentially distributed in matte, and lower matte grades and adding CaO and Al₂O₃ favored their department into matte. In contrast, iron was highly deported into slags with the increasing matte grade. The equilibrium slag compositions measured in the present study indicate the operating area for designing industrial smelting slags. The slag compositions could be regulated by adjusting the Fe/SiO₂ ratio and mass fractions of CaO and Al₂O₃ in slags to reduce the proportions of solids in the slag or obtain a fully molten slag. This study enriches fundamental data for optimizing WEEE smelting operations and improving metal recovery efficiency toward sustainable use of metals.

Author Contributions: Conceptualization, methodology, formal analysis, investigation, and data curation: M.T. and Q.W. (Qiongqiong Wang); writing—original draft preparation: M.T.; review and editing: S.W. and X.W.; funding acquisition: S.W., Q.W. (Qinmeng Wang), and X.G. All authors have read and agreed to the published version of the manuscript.

Funding: This research was funded by the National Key Research and Development Program of China, grant number 2022YFC3901501, and the National Natural Science Foundation of China, grant numbers U20A20273 and 52304377.

Institutional Review Board Statement: Not applicable.

Informed Consent Statement: Not applicable.

Data Availability Statement: Data are contained within the article.

Conflicts of Interest: The authors declare no conflicts of interest.

References

1. Cucchiella, F.; D'Adamo, I.; Lenny Koh, S.C.; Rosa, P. Recycling of WEEEs: An Economic Assessment of Present and Future e-Waste Streams. *Renew. Sustain. Energy Rev.* **2015**, *51*, 263–272. [[CrossRef](#)]
2. Cui, J.; Zhang, L. Metallurgical Recovery of Metals from Electronic Waste: A Review. *J. Hazard. Mater.* **2008**, *158*, 228–256. [[CrossRef](#)]
3. Yang, C.; Wu, H.; Cai, M.; Zhou, Y.; Guo, C.; Han, Y.; Zhang, L. Valorization of Biomass-Derived Polymers to Functional Biochar Materials for Supercapacitor Applications via Pyrolysis: Advances and Perspectives. *Polymers* **2023**, *15*, 2741. [[CrossRef](#)] [[PubMed](#)]
4. Hagelüken, C. Recycling of Electronic Scrap at Umicore's Integrated Metals Smelter and Refinery. *World Metall.* **2006**, *59*, 152–161.

5. Avarmaa, K.; Yliaho, S.; Taskinen, P. Recoveries of Rare Elements Ga, Ge, In and Sn from Waste Electric and Electronic Equipment through Secondary Copper Smelting. *Waste Manag.* **2018**, *71*, 400–410. [[CrossRef](#)]
6. Mackey, P.J. The Physical Chemistry of Copper Smelting Slags—a Review. *Can. Metall. Q.* **1982**, *21*, 221–260. [[CrossRef](#)]
7. Anindya, A.; Swinbourne, D.R.; Reuter, M.A.; Matusewicz, R.W. Distribution of Elements between Copper and FeO_x-CaO-SiO₂ Slags during Pyrometallurgical Processing of WEEE. *Miner. Process. Extr. Metall.* **2013**, *122*, 165–173. [[CrossRef](#)]
8. Sineva, S.; Hayes, P.C.; Jak, E. Experimental Study of the Slag/Matte/Metal (Fe or Cu)/Tridymite Equilibria in the Cu-Fe-O-S-Si-(Ca) System at 1473K (1200 °C): Effect of Ca. *Met. Mater. Trans B* **2021**, *52*, 2163–2170. [[CrossRef](#)]
9. Fallah-Mehrjardi, A.; Hayes, P.C.; Jak, E. The Effect of CaO on Gas/Slag/Matte/Tridymite Equilibria in Fayalite-Based Copper Smelting Slags at 1473 K (1200 °C) and P(SO₂) = 0.25 Atm. *Met. Mater. Trans B* **2018**, *49*, 602–609. [[CrossRef](#)]
10. Sineva, S.; Fallah-Mehrjardi, A.; Hidayat, T.; Shevchenko, M.; Shishin, D.; Hayes, P.C.; Jak, E. Experimental Investigation of Gas/Slag/Matte/Tridymite Equilibria in the Cu-Fe-O-S-Si-Al-Ca-Mg System in Controlled Gas Atmosphere: Experimental Results at 1473 K (1200 °C), 1573 K (1300 °C) and p(SO₂) = 0.25 Atm. *J. Phase Equilib. Diffus.* **2020**, *41*, 243–256. [[CrossRef](#)]
11. Sineva, S.; Fallah-Mehrjardi, A.; Hidayat, T.; Hayes, P.C.; Jak, E. Experimental Study of the Individual Effects of Al₂O₃, CaO and MgO on Gas/Slag/Matte/Spinel Equilibria in Cu-Fe-O-S-Si-Al-Ca-Mg System at 1473K (1200 °C) and P(SO₂) = 0.25 Atm. *J. Phase Equilib. Diffus.* **2020**, *41*, 859–869. [[CrossRef](#)]
12. Chen, M.; Avarmaa, K.; Taskinen, P.; Michallik, R.; Jokilaakso, A. Investigation on the Matte/Slag/Spinel/Gas Equilibria in the Cu-Fe-O-S-SiO₂-(CaO, Al₂O₃) System at 1250 °C and pSO₂ of 0.25 Atm. *Miner. Process. Extr. Metall. Rev.* **2022**, *44*, 313–324. [[CrossRef](#)]
13. Chen, M.; Avarmaa, K.; Taskinen, P.; Klemettinen, L.; Michallik, R.; O'Brien, H.; Jokilaakso, A. Novel Fluxing Strategy of Copper Matte Smelting and Trace Metals in E-Waste Recycling. *Miner. Eng.* **2023**, *191*, 107969. [[CrossRef](#)]
14. Sun, Y.; Chen, M.; Balladares, E.; Pizarro, C.; Contreras, L.; Zhao, B. Effect of CaO on the Liquid/Spinel/Matte/Gas Equilibria in the Si-Fe-O-Cu-S System at Controlled P(SO₂) 0.3 and 0.6 Atm. *Calphad* **2020**, *69*, 101751. [[CrossRef](#)]
15. Chen, M.; Avarmaa, K.; Klemettinen, L.; Shi, J.; Taskinen, P.; Jokilaakso, A. Experimental Study on the Phase Equilibrium of Copper Matte and Silica-Saturated FeO_x-SiO₂-Based Slags in Pyrometallurgical WEEE Processing. *Met. Mater. Trans. B* **2020**, *51*, 1552–1563. [[CrossRef](#)]
16. Chen, M.; Avarmaa, K.; Klemettinen, L.; Shi, J.; Taskinen, P.; Lindberg, D.; Jokilaakso, A. Equilibrium of Copper Matte and Silica-Saturated Iron Silicate Slags at 1300 °C and PSO₂ of 0.5 Atm. *Met. Mater. Trans. B* **2020**, *51*, 2107–2118. [[CrossRef](#)]
17. Sukhomlinov, D.; Klemettinen, L.; O'Brien, H.; Taskinen, P.; Jokilaakso, A. Behavior of Ga, In, Sn, and Te in Copper Matte Smelting. *Met. Mater. Trans. B* **2019**, *50*, 2723–2732. [[CrossRef](#)]
18. Heo, J.H.; Park, S.-S.; Park, J.H. Effect of Slag Composition on the Distribution Behavior of Pb between Fe_tO-SiO₂-(CaO, Al₂O₃) Slag and Molten Copper. *Met. Mater. Trans. B* **2012**, *43*, 1098–1105. [[CrossRef](#)]
19. Kim, H.G.; Sohn, H.Y. Effects of CaO, Al₂O₃, and MgO Additions on the Copper Solubility, Ferric/Ferrous Ratio, and Minor-Element Behavior of Iron-Silicate Slags. *Met. Mater. Trans. B* **1998**, *29*, 583–590. [[CrossRef](#)]
20. Tian, M.; Wang, Q.; Wang, Q.; Li, W.; Guo, X. Effect of MgO on Phase Equilibria of Copper Matte and SiO₂-Saturated Iron Silicate Slag in Smelting Complicated Copper Resources. *Trans. Nonferrous Met. Soc. China* **2023**, *33*, 3544–3559. [[CrossRef](#)]
21. Yazawa, A. Thermodynamic Considerations of Copper Smelting. *Can. Metall. Q.* **1974**, *13*, 443–453. [[CrossRef](#)]
22. Abdeyazdan, H.; Fallah-Mehrjardi, A.; Hidayat, T.; Shevchenko, M.; Hayes, P.C.; Jak, E. The Effect of MgO on Gas-Slag-Matte-Tridymite Equilibria in Fayalite-Based Copper Smelting Slags at 1473 K (1200 °C) and 1573 K (1300 °C), and P(SO₂) = 0.25 Atm. *J. Phase Equilib. Diffus.* **2020**, *41*, 44–55. [[CrossRef](#)]
23. Sineva, S.; Shishin, D.; Shevchenko, M.; Hayes, P.C.; Jak, E. Experimental Study of the Combined Effects of Al₂O₃, CaO and MgO on Gas/Slag/Matte/Spinel Equilibria in the Cu-Fe-O-S-Si-Al-Ca-Mg System at 1473K (1200 °C) and p(SO₂) = 0.25 Atm. *J. Sustain. Metall.* **2023**, *9*, 599–612. [[CrossRef](#)]
24. Nagamori, M.; Mackey, P.J. Thermodynamics of Copper Matte Converting: Part I. Fundamentals of the Noranda Process. *Metall. Trans. B* **1978**, *9*, 255–265. [[CrossRef](#)]
25. Wang, Q.; Guo, X.; Wang, S.; Liao, L.; Tian, Q. Multiphase Equilibrium Modeling of Oxygen Bottom-Blown Copper Smelting Process. *Trans. Nonferrous Met. Soc. China* **2017**, *27*, 2503–2511. [[CrossRef](#)]
26. Matusewicz, R.W.; Reuter, M.A.; Hughes, S.P.; Lin, S.; Sun, L. Large Scale Copper Smelting Using Ausmelt TSL Technology at the Tongling Jinchang Smelter. In Proceedings of the Copper 2010, Hamburg, Germany, 6–10 June 2010; Volume 3, pp. 961–970.
27. Shishin, D.; Hidayat, T.; Fallah-Mehrjardi, A.; Hayes, P.C.; Dectero, S.A.; Jak, E. Integrated Experimental and Thermodynamic Modeling Study of the Effects of Al₂O₃, CaO, and MgO on Slag-Matte Equilibria in the Cu-Fe-O-S-Si-(Al, Ca, Mg) System. *J. Phase Equilib. Diffus.* **2019**, *40*, 445–461. [[CrossRef](#)]
28. Henao, H.M.; Nexhip, C.; George-Kennedy, D.P.; Hayes, P.C.; Jak, E. Investigation of Liquidus Temperatures and Phase Equilibria of Copper Smelting Slags in the FeO-Fe₂O₃-SiO₂-CaO-MgO-Al₂O₃ System at PO₂ 10⁻⁸ Atm. *Met. Mater. Trans. B* **2010**, *41*, 767–779. [[CrossRef](#)]
29. Hidayat, T.; Fallah-Mehrjardi, A.; Hayes, P.C.; Jak, E. Experimental Investigation of Gas/Slag/Matte/Spinel Equilibria in the Cu-Fe-O-S-Si System at 1473K (1200 °C) and P(SO₂) = 0.25 Atm. *Met. Mater. Trans B* **2018**, *49*, 1750–1765. [[CrossRef](#)]

Disclaimer/Publisher's Note: The statements, opinions and data contained in all publications are solely those of the individual author(s) and contributor(s) and not of MDPI and/or the editor(s). MDPI and/or the editor(s) disclaim responsibility for any injury to people or property resulting from any ideas, methods, instructions or products referred to in the content.